

Synthesis and Reactions of Cubane-Type Iron–Sulfur–Phosphine Clusters, Including Soluble Clusters of Nuclearities 8 and 16

Hong-Cai Zhou and R. H. Holm*

Department of Chemistry and Chemical Biology, Harvard University,
Cambridge, Massachusetts 02138

Received July 19, 2002

A family of soluble, reduced iron–sulfur clusters with nuclearities 4, 8, and 16 having tertiary phosphine ligation and based on the Fe_4S_4 cubane-type structural motif has been synthesized. The results of this investigation substantially extend and improve the results of our original work on iron–sulfur–phosphine clusters (Goh, C.; Segal, B. M.; Huang, J.; Long, J. R.; Holm, R. H. *J. Am. Chem. Soc.* **1996**, *118*, 11844). A general property of this cluster family is facile phosphine substitution. The clusters $[\text{Fe}_4\text{S}_4(\text{PR}_3)_4]^+$ are precursors to monosubstituted $[\text{Fe}_4\text{S}_4(\text{PR}_3)_3\text{X}]$ ($\text{X} = \text{Cl}^-$, RS^-), homoleptic $[\text{Fe}_4\text{S}_4(\text{SR})_4]^{3-}$, and all-ferrous monocubanes $[\text{Fe}_4\text{S}_4(\text{PR}_3)_4]$ ($\text{R} = \text{Pr}^i$, Cy , Bu^i ; generated in solution). In turn, $[\text{Fe}_4\text{S}_4(\text{PPr}^i)_3(\text{SSiPh}_3)]$ and $[\text{Fe}_4\text{S}_4(\text{PPr}^i)_4]$ can be transformed into the dicubanes $[\text{Fe}_8\text{S}_8(\text{PPr}^i)_4(\text{SSiPh}_3)_2]$ and $[\text{Fe}_8\text{S}_8(\text{PPr}^i)_6]$, respectively. Further, the tetracubanes $[\text{Fe}_{16}\text{S}_{16}(\text{PR}_3)_8]$ are also accessible from $[\text{Fe}_4\text{S}_4(\text{PR}_3)_4]$ under different conditions. X-ray structures are described for $[\text{Fe}_4\text{S}_4(\text{PCy}_3)_3\text{X}]$ ($\text{X} = \text{Cl}^-$, PhS^-), $[\text{Fe}_8\text{S}_8(\text{PPr}^i)_4(\text{SSiPh}_3)_2]$, $[\text{Fe}_8\text{S}_8(\text{PPr}^i)_6]$, and $[\text{Fe}_{16}\text{S}_{16}(\text{PCy}_3)_8]$. The monosubstituted clusters show different distortions of the $[\text{Fe}_4\text{S}_4]^+$ cores from idealized cubic symmetry. The dicubanes possess edge-bridged double cubane structures with an $\text{Fe}_2(\mu_4\text{-S})_2$ bridge rhomb and idealized C_{2h} symmetry. The ready cleavage of these clusters into single cubanes is considered a probable consequence of strained bond angles at the $\mu_4\text{-S}$ atoms. Tetracubanes contain four individual cubanes, each of which is implicated in two bridge rhombs so as to generate a cyclic structure of idealized D_4 symmetry. Redox properties and Mössbauer spectroscopic parameters are reported. The species $[\text{Fe}_4\text{S}_4(\text{PR}_3)_4]$ (in solution), $[\text{Fe}_8\text{S}_8(\text{PR}_3)_6]$, and $[\text{Fe}_{16}\text{S}_{16}(\text{PR}_3)_8]$ are the only synthetic all-ferrous clusters with tetrahedral iron sites that have been isolated. Their utility as precursors to other highly reduced iron–sulfur clusters is under investigation.

Introduction

It is increasingly evident that iron–sulfur and hetero-metal–iron–sulfur clusters with the majority or all of the iron atoms in the Fe^{II} state present structural and reactivity properties not manifested by more oxidized clusters. Early examples of this behavior with iron–sulfur clusters include the variable spin states and multiplicity of distortions of the $[\text{Fe}_4\text{S}_4]^+$ core in $[\text{Fe}_4\text{S}_4(\text{SR})_4]^{3-}$ ($\text{Fe}^{2.25+}$) from idealized cubic symmetry^{1–3} compared to the usual (but not invariant) compressed tetragonal geometry of $[\text{Fe}_4\text{S}_4]^{2+}$ ($\text{Fe}^{2.5+}$) cores

and the facile exchange of core chalcogenide atoms in the systems $[\text{Fe}_4\text{S}_4(\text{SR})_4]^{3-}/[\text{Fe}_4\text{Se}_4(\text{SR})_4]^{3-}$ in contrast to the very slow exchange between dinegative clusters.⁴ In the same period, it was shown that tertiary phosphines are effective in stabilizing highly reduced clusters, including those not obtained with conventional thiolate or halide terminal ligation. Examples are the “basket” clusters $[\text{Fe}_6\text{S}_6(\text{PR}_3)_4\text{L}_2]$ ($\text{Fe}^{2.33+}$, $\text{L} = \text{halide}$, RS^-)^{5,6} and $[\text{Fe}_6\text{S}_6(\text{PET}_3)_6]^{1+}$ ($\text{Fe}^{2.17+}$)⁷ and the monocapped prismane $[\text{Fe}_7\text{S}_6(\text{PET}_3)_4\text{Cl}_3]$ ($\text{Fe}^{2.14+}$).⁸ More recently, the cubane-type clusters $[\text{Fe}_4\text{S}_4(\text{PR}_3)_4]^{+9}$ and

* To whom correspondence should be addressed. E-mail: holm@chemistry.harvard.edu.

- (1) Carney, M. J.; Papaefthymiou, G. C.; Spartalian, K.; Frankel, R. B.; Holm, R. H. *J. Am. Chem. Soc.* **1988**, *110*, 6084–6095.
- (2) Carney, M. J.; Papaefthymiou, G. C.; Whitener, M. A.; Spartalian, K.; Frankel, R. B.; Holm, R. H. *Inorg. Chem.* **1988**, *27*, 346–352.
- (3) Carney, M. J.; Papaefthymiou, G. C.; Frankel, R. B.; Holm, R. H. *Inorg. Chem.* **1989**, *28*, 1497–1503.

- (4) Reynolds, J. G.; Holm, R. H. *Inorg. Chem.* **1981**, *20*, 1873–1878.
- (5) Snyder, B. S.; Holm, R. H. *Inorg. Chem.* **1988**, *27*, 2339–2347.
- (6) Reynolds, M. S.; Holm, R. H. *Inorg. Chem.* **1988**, *27*, 4494–4499.
- (7) Snyder, B. S.; Holm, R. H. *Inorg. Chem.* **1990**, *29*, 274–279.
- (8) Noda, I.; Snyder, B. S.; Holm, R. H. *Inorg. Chem.* **1986**, *25*, 3851–3853.
- (9) Goh, C.; Segal, B. M.; Huang, J.; Long, J. R.; Holm, R. H. *J. Am. Chem. Soc.* **1996**, *118*, 11844–11853.

$[\text{Fe}_4\text{S}_4(\text{PR}_3)_3\text{L}]^{10}$ (both $\text{Fe}^{2.25+}$) have been prepared (L = halide).

An expanding number of reduced heterometal clusters are stabilized by tertiary phosphines. These include the single cubanes $[(\text{Cl}_4\text{cat})(\text{MeCN})\text{MoFe}_3\text{S}_4(\text{PR}_3)_3]^{11}$ and $[(\text{HB}(\text{pz})_3)\text{VFe}_3\text{S}_4(\text{PET}_3)_3]^{+12}$ (both $\text{Fe}^{2.33+}$), the edge-bridged double cubanes $[(\text{Cl}_4\text{cat})_2\text{L}_2\text{Mo}_2\text{Fe}_6\text{S}_8(\text{PR}_3)_4]$ (L = MeCN, PR_3)^{11,13,14} and $[(\text{HB}(\text{pz})_3)_2\text{V}_2\text{Fe}_6\text{S}_8(\text{PET}_3)_4]$,¹² and an interesting variety of other Mo–Fe–S clusters carrying phosphine and carbonyl ligands.^{14–17} Some of these clusters have an MoFe_3S_3 subunit whose cuboidal shape resembles a fragment of the iron–molybdenum cofactor cluster of nitrogenase. Edge-bridged double cubanes are synthetic precursors to larger clusters with $\text{Mo}_2\text{Fe}_6\text{S}_9$ fragments^{18,19} and individual clusters with $\text{M}_2\text{Fe}_6\text{S}_9$ cores (M = V, Mo),²⁰ these species having dominant Fe^{II} character and a structure closely related to the P^{N} cluster of nitrogenase.

In a biological content, all-ferrous clusters are of considerable current interest because of the recent discovery that the cluster of the iron protein of nitrogenase can exist in the $[\text{Fe}_4\text{S}_4]^0$ state^{21–24} in addition to the more conventional $[\text{Fe}_4\text{S}_4]^{2+,+}$ oxidation levels. From protein crystallography, the fully reduced cluster occurs as $\text{Fe}_4\text{S}_4(\text{S}\cdot\text{Cys})_4$ with a cubane-type core of unexceptional dimensions.²⁵ Other all-ferrous clusters are the edge-bridged dicubane $[\text{Fe}_8\text{S}_8(\text{PCy}_3)_6]^{9,26}$ and tetracubanes $[\text{Fe}_{16}\text{S}_{16}(\text{PR}_3)_8]^{9,26}$ and octanuclear $[\text{Fe}_8\text{S}_6\text{I}_8]^{4–27}$ and $[\text{Fe}_8\text{S}_6(\text{PCy}_3)_4\text{Cl}_4]$,⁹ whose cores have idealized O_h symmetry. We exclude from further consideration $[\text{Fe}_4\text{S}_4(\text{CO})_{12}]^{28}$ whose six-coordinate diamagnetic Fe^{II} sites separated by ca. 3.4 Å place it in a class of closed-shell clusters. In this work, we have reexamined, clarified, and extended the chemistry of reduced cubane-type $[\text{Fe}_4\text{S}_4]$ clusters with tertiary phosphine ligation and their edge-

bridged oligomers. The synthesis and interconversion of these species have been systematized, allowing simpler entry to this class of clusters with nuclearities 4, 8, and 16.

Experimental Section

Preparation of Compounds. All operations were conducted under a pure dinitrogen atmosphere using an inert-atmosphere box or standard Schlenk techniques. Solvents were passed through an Innovative Technology solvent purification system prior to use. The compounds $[\text{Fe}(\text{PET}_3)_2\text{Cl}_2]$, $(\text{Ph}_4\text{P})_2[\text{Fe}_4\text{S}_4\text{Cl}_4]$, $[\text{Fe}_4\text{S}_4(\text{PCy}_3)_4](\text{BPh}_4)$, and $[\text{Fe}_4\text{S}_4(\text{P}^i\text{Bu})_4](\text{BPh}_4)$ were prepared as described.⁹ Other compounds were of commercial origin and used as received. New or improved syntheses for $[\text{Fe}_4\text{S}_4(\text{P}^i\text{Pr})_4](\text{BPh}_4)$ and $[\text{Fe}_{16}\text{S}_{16}(\text{PR}_3)_8]$ (R = Prⁱ, Cy, Bu^t)⁹ are given below. Solvent reduction steps were performed in vacuo.

(Ph₄P)(SPh). A solution of Ph_4PCl (0.375 g, 1.00 mmol) in 5 mL of acetonitrile was treated with a slurry of NaSPh (0.132 g, 1.00 mmol) in 5 mL of acetonitrile. A pale yellow suspension appeared immediately. The mixture was stirred for 30 min and filtered through a Celite column. The filtrate was layered with ether (50 mL), and the mixture was allowed to stand overnight. Light yellow needle-shaped crystals were collected, washed with ether (3 × 5 mL), and dried in vacuo to afford 0.361 g (81%) of product. ¹H NMR (CD_3CN): δ 6.48 (1, t), 6.70 (2, t), 7.13 (2, d), 7.70 (16, m), 7.90 (4, t).

(Ph₄P)(SSiPh₃). A solution of NaSSiPh_3 ²⁹ (0.386 g, 1.23 mmol) in 15 mL of acetonitrile was added to a solution of Ph_4PBr (0.459 g, 1.10 mmol) in 15 mL of acetonitrile. A white precipitate formed immediately. The mixture was stirred for 2 h and filtered through a Celite plug to remove a fine white solid. The filtrate was concentrated to 15 mL and layered with ether (100 mL), and the mixture was allowed to stand overnight. The solid was collected, washed with ether (3 × 5 mL), and dried in vacuo to afford the product as 0.508 g (73%) of white shiny flakes. ¹H NMR (CD_3CN): δ 7.16 (9, m), 7.65–7.76 (22, m), 7.91 (4, m).

$[\text{Fe}_4\text{S}_4(\text{P}^i\text{Pr})_4](\text{BPh}_4)$. Black crystalline $(\text{Ph}_4\text{P})_2[\text{Fe}_4\text{S}_4\text{Cl}_4]$ (5.8 g, 5.0 mmol) was dispersed in 20 mL of acetonitrile. A solution of P^iPr_3 (4.4 mL, 23 mmol) in 20 mL of THF was added followed by a solution of NaBPh_4 (6.8 g, 20 mmol) in 10 mL of acetonitrile. The dark brown suspension was stirred for 1 h and mixed thoroughly with 50 mL of ether. The mixture was filtered to remove a white solid, the filtrate was reduced to dryness, and the solid residue was extracted with THF (2 × 10 mL). To the extract was added 200 mL of ether, causing separation of a black solid. The supernatant was decanted, and the crystals were washed extensively with ether and dried to afford the product as 5.6 g (85%) of black rhombic plates. ¹H NMR (CD_3CN , anion): δ 2.29 (CH_3), 5.05 (CH). Anal. Calcd for $\text{C}_{60}\text{H}_{104}\text{BF}_4\text{P}_4\text{S}_4$: C, 54.94; H, 7.99; Fe, 17.03; P, 9.44; S, 9.78. Found: C, 54.78; H, 7.89; Fe, 17.15; P, 9.40; S, 9.79.

$[\text{Fe}_4\text{S}_4(\text{PCy}_3)_3\text{Cl}]\cdot\text{MeCN}$. To a dark brown solution of $[\text{Fe}_4\text{S}_4(\text{PCy}_3)_4](\text{BPh}_4)$ (0.50 g, 0.28 mmol) in 10 mL of dichloromethane was added a solution of Ph_4PCl (0.13 g, 0.35 mmol) in 10 mL of dichloromethane. The color of the mixture darkened to black, and a colorless solid appeared after 5 min of stirring. The mixture was filtered; the brown-black filtrate was taken to dryness overnight. The black residue was extracted with toluene (2 × 5 mL). The extract was evaporated, resulting in a black solid which was extracted with THF (2 × 5 mL). The extract was layered with

- (10) Tyson, M. A.; Demadis, K. D.; Coucouvanis, D. *Inorg. Chem.* **1995**, *34*, 4519–4520.
 (11) Osterloh, F.; Segal, B. M.; Achim, C.; Holm, R. H. *Inorg. Chem.* **2000**, *39*, 980–989.
 (12) Hauser, C.; Bill, E.; Holm, R. H. *Inorg. Chem.* **2002**, *41*, 1615–1624.
 (13) Demadis, K. D.; Campana, C. F.; Coucouvanis, D. *J. Am. Chem. Soc.* **1995**, *117*, 7832–7833.
 (14) Han, J.; Koutmos, M.; Al-Ahmad, S.; Coucouvanis, D. *Inorg. Chem.* **2001**, *40*, 5985–5999.
 (15) Han, J.; Beck, K.; Ockwig, N.; Coucouvanis, D. *J. Am. Chem. Soc.* **1999**, *121*, 10448–10449.
 (16) Han, J.; Coucouvanis, D. *J. Am. Chem. Soc.* **2001**, *123*, 11304–11305.
 (17) Coucouvanis, D.; Han, J.; Moon, N. *J. Am. Chem. Soc.* **2002**, *124*, 216–224.
 (18) Osterloh, F.; Sanakis, Y.; Staples, R. J.; Münck, E.; Holm, R. H. *Angew. Chem., Int. Ed. Engl.* **1999**, *38*, 2066–2070.
 (19) Osterloh, F.; Achim, C.; Holm, R. H. *Inorg. Chem.* **2001**, *40*, 224–232.
 (20) Zhang, Y.; Zuo, J.-L.; Zhou, H.-C.; Holm, R. H. *J. Am. Chem. Soc.* **2002**, *124*, 14292–14293.
 (21) Watt, G. D.; Reddy, K. R. N. *J. Inorg. Biochem.* **1994**, *53*, 281–294.
 (22) Musgrave, K. B.; Angove, H. C.; Burgess, B. K.; Hedman, B.; Hodgson, K. O. *J. Am. Chem. Soc.* **1998**, *120*, 5325–5326.
 (23) Yoo, S. J.; Angove, H. C.; Burgess, B. K.; Hendrich, M. P.; Münck, E. *J. Am. Chem. Soc.* **1999**, *121*, 2534–2545.
 (24) Angove, H. C.; Yoo, S. J.; Burgess, B. K.; Münck, E. *J. Am. Chem. Soc.* **1997**, *119*, 8730–8731.
 (25) Strop, P.; Takahara, P. M.; Chiu, H.-J.; Angove, H. C.; Burgess, B. K.; Rees, D. C. *Biochemistry* **2001**, *40*, 651–656.
 (26) Cai, L.; Segal, B. M.; Long, J. R.; Scott, M. J.; Holm, R. H. *J. Am. Chem. Soc.* **1995**, *117*, 8863–8864.
 (27) Pohl, S.; Opitz, U. *Angew. Chem., Int. Ed. Engl.* **1993**, *32*, 863–864.
 (28) Nelson, L. L.; Lo, F. Y. K.; Rae, A. D.; Dahl, L. F. *J. Organomet. Chem.* **1982**, *225*, 309–329.

- (29) Chadwick, S.; Englich, U.; Ruhlandt-Senge, K. *Organometallics* **1997**, *16*, 5792–5803.

acetonitrile (35 mL). The mixture was allowed to stand overnight, affording the product as 0.17 g (48%) of black blocklike crystals. EPR (5 K, toluene/dichloromethane (1:1 v/v)): $g_{\perp} = 1.96$, $g_{\parallel} = 2.13$. Anal. Calcd for $C_{56}H_{102}ClFe_4NP_3S_4$: C, 52.99; H, 8.10; N, 1.10; P, 7.32; S, 10.10. Found: C, 53.09; H, 8.18; N, 1.15; P, 7.26; S, 10.04. The compound was further identified by an X-ray structure determination.

[Fe₄S₄(PCy₃)₃(SPh)]. To a solution of [Fe₄S₄(PCy₃)₄](BPh₄) (0.22 g, 0.12 mmol) in 8 mL of THF was added a solution of (Ph₄P)(SPh) (0.60 g, 0.13 mmol) in 6 mL of acetonitrile. The reaction mixture was stirred overnight; the dark brown suspension was filtered to remove a gray solid. The filtrate was reduced to dryness, and the black residue was extracted with toluene (3 × 2 mL). Solvent was removed from the combined extracts to give a black solid, which was dissolved in THF (6 mL). The solution was layered with acetonitrile (12 mL). The product was obtained as 0.050 g (32%) of black block-shaped crystals after 3 d. ¹H NMR (CD₂Cl₂): δ 12.2 (*m*-H), 3.14 (CH), 1.45–2.72 (CH₂), –1.51 (*br*, *o*-H), –1.75 (*p*-H). The compound was further identified by an X-ray structure determination.

[Fe₄S₄(PPr^{*i*})₃(SPh)].³⁰ A solution of [Fe(PEt₃)₂Cl₂] (5.00 g, 13.8 mmol) in 50 mL of toluene was treated with solid NaSPh (3.60 g, 27.3 mmol), producing immediately a white solid and dark red suspension. The mixture was stirred for 1 h and twice filtered through a 1 in. bed of Celite to remove a finely divided solid. To the dark red filtrate, (PhCH₂S)₂S (5.75 g, 20.7 mmol) was added followed by PPr^{*i*} (5.00 g, 31.2 mmol). The mixture was stirred for 4 h and filtered. The filtrate was concentrated in vacuo to ca. 20 mL, layered with 200 mL of acetonitrile, and maintained at –20 °C for 4 d. The product was isolated as 1.22 g (38%) of long black prismatic crystals. ¹H NMR (C₆D₆): δ 13.15 (*m*-H), 3.07 (*br*, CH), 1.97 (*br*, CH₃), –1.65 (*br*, *o*-H), –2.77 (*p*-H). Anal. Calcd for C₃₃H₆₈Fe₄P₃S₅: C, 42.10; H, 7.28; Fe, 23.73; P, 9.87; S, 17.03. Found: C, 41.89; H, 7.32; Fe, 23.84; P, 9.87; S, 17.02.

[Fe₄S₄(PPr^{*i*})₃(SSiPh₃)]. To a solution of [Fe₄S₄(PPr^{*i*})₄](BPh₄) (0.26 g, 0.20 mmol) in 30 mL of THF was added a solution of (Ph₄P)(SSiPh₃) (0.13 g, 0.21 mmol) in 30 mL of acetonitrile. The dark reddish-brown suspension was stirred for 1 h and filtered through Celite. The dark brown filtrate was taken to dryness overnight, the residue was extracted with THF (2 × 2 mL), and solvent was removed. The residue was washed with small quantities of acetonitrile and ether and dried to give the product as 0.19 g (~85%) of a black solid. ¹H NMR (C₆D₆): δ 8.30 (*m*-H), 7.64 (*o*-H), 7.27 (*p*-H), 3.06 (CH), 1.94 (CH₃).

[Fe₈S₈(PPr^{*i*})₄(SSiPh₃)₂]. [Fe₄S₄(PPr^{*i*})₃(SSiPh₃)] (0.22 g, 0.20 mmol) was dissolved in 6 mL of THF. Ether vapor diffusion overnight gave a black crystalline solid, which was collected, washed with acetonitrile, toluene, and ether (all 3 × 5 mL) and dried. The product was obtained as 0.14 g (73%) of black rectangular plates. ¹H NMR (CD₂Cl₂): δ 7.59 (*vbr*, CH), 7.20 (*o*-, *p*-H), 6.69 (*m*-H), 3.21 (*br*, CH₃). Anal. Calcd for C₇₂H₁₁₄Fe₈P₄S₁₀-Si₂: C, 44.87; H, 5.96; Fe, 23.18; P, 6.43; S, 16.64. Found: C, 44.96; H, 6.09; Fe, 23.07; P, 6.56; S, 16.52. This compound was further identified by an X-ray structure determination.

[Fe₄S₄(PPr^{*i*})₄]. To a dark brown solution of [Fe₄S₄(PPr^{*i*})₄](BPh₄) (0.43 g, 0.33 mmol) and PPr^{*i*} (1.5 mL, 7.7 mmol) in 2 mL of THF was added a freshly prepared solution of potassium benzophenone ketyl (0.36 mmol) in 3 mL of THF. A reddish black suspension formed instantaneously. A pale-colored solid was removed by filtration, to afford a solution of the title compound. FAB⁺ MS (*m/e*): M⁺ (990), M⁺ – PPr^{*i*} (831), M⁺ – 2PPr^{*i*} (671),

M⁺ – 3PPr^{*i*} (511), Fe₄S₄ (351). Absorption spectrum (THF): λ_{\max} (ϵ_M) 567 (sh, 2070) nm. Multiple attempts to isolate this compound in substance failed.

[Fe₈S₈(PPr^{*i*})₆]. A solution of [Fe₄S₄(PPr^{*i*})₄] (0.28 mmol, based on [Fe₄S₄(PPr^{*i*})₄](BPh₄)) in 2 mL of THF containing 1.5 mL (7.7 mmol) of PPr^{*i*} was layered with a solution of PPr^{*i*} (1 mL, 5.1 mmol) in 12 mL of acetonitrile. The reaction mixture was allowed to stand for 3 d. The solid was collected, washed with acetonitrile and ether (each 3 × 5 mL), and dried to yield the product as 0.14 g (60%) of black blocklike crystals. Absorption spectrum (benzene): λ_{\max} (ϵ_M) 572 (8080) nm. ¹H NMR (C₆D₆): δ 14.3 (2, CH), 3.57 (18, CH₃), 3.45 (18, CH₃), –0.16 (18, CH₃), –2.11 (1, CH). Anal. Calcd for C₅₄H₁₂₆Fe₈P₆S₈: C, 38.96; H, 7.63; Fe, 26.84; P, 11.16; S, 15.41. Found: C, 39.12; H, 7.74; Fe, 26.91; P, 11.25; S, 15.46. This compound is soluble in benzene and toluene and is slightly soluble in THF. It was further identified by an X-ray structure determination.

[Fe₁₆S₁₆(PPr^{*i*})₈]. A freshly prepared solution of potassium benzophenone ketyl (0.60 mmol) in 30 mL of THF was added to a stirred solution of [Fe₄S₄(PPr^{*i*})₄](BPh₄) (0.67 g, 0.51 mmol) and PPr^{*i*} (0.22 mL, 1.1 mmol) in 20 mL of THF. The reaction mixture was stirred for 30 min and filtered to remove a pale-colored solid. The filtrate was carefully layered with a solution of PPr^{*i*} (0.27 mL, 1.4 mmol) in 500 mL of acetonitrile. The mixture was allowed to stand for 3 d, and the dark brown supernatant was decanted to leave black crystals. These were washed extensively with acetonitrile and dried to afford the product as 0.060 g of black rhombic crystals. A second crop was obtained by reducing the volume of the supernatant to ca. 5 mL. The two crops of crystals were combined to give 0.19 g (55%) of product. Absorption spectrum (benzene): λ_{\max} (ϵ_M) 544 (20 400) nm. ¹H NMR (C₆D₆): δ 3.70 (1, CH), 1.54 (3, CH₃), 1.18 (3, CH₃). Anal. Calcd for C₇₂H₁₆₈-Fe₁₆P₈S₁₆: C, 32.17; H, 6.30; Fe, 33.24; P, 9.22; S, 19.08. Found: C, 32.21; H, 6.21; Fe, 33.21; P, 9.21; S, 19.14. This compound is soluble in benzene and toluene and moderately soluble in THF. It was further identified by comparison of cell parameters of the diacetonitrile solvate⁹ and by a full structure determination in this work.

[Fe₁₆S₁₆(PCy₃)₈]. A freshly prepared solution of potassium benzophenone ketyl (0.58 mmol) in 14 mL of THF was added to a stirred solution of [Fe₄S₄(PCy₃)₄](BPh₄) (0.97 g, 0.54 mmol) and PCy₃ (2.0 g, 7.1 mmol) in 12 mL of THF. The black solution was filtered; the filtrate was carefully layered with 24 mL of acetonitrile and allowed to stand for 3 d. The crystalline solid was collected, washed with acetonitrile, THF, and ether and dried. The product was obtained as 0.22 g (45%) of shiny dark brown crystals. It was identified by an X-ray structure determination. The compound is very sparingly soluble in benzene, toluene, and THF.

[Fe₁₆S₁₆(PBU^{*t*})₈]. A freshly prepared solution of potassium benzophenone ketyl (0.31 mmol) in 10 mL of THF was added to a solution of [Fe₄S₄(PBU^{*t*})₄](BPh₄) (0.44 g, 0.30 mmol) and PBU^{*t*} (0.50 g, 2.5 mmol) in 10 mL of THF. The reaction mixture was stirred for 30 min, the black suspension was filtered, and the filtrate was carefully layered with 10 mL of acetonitrile. After 7 d a solid was collected, washed extensively with acetonitrile, and dried to give the product as 0.14 g (62%) of a brown solid. Absorption spectrum (THF): λ_{\max} (ϵ_M) 558 (18 000) nm. ¹H NMR (C₆D₆): δ 1.90. This compound is soluble in benzene, toluene, and THF. It has previously been identified by X-ray structure determination.⁹

(Et₄N)₃[Fe₄S₄(SPh)₄]. To a black solution of [Fe₄S₄(PPr^{*i*})₄](BPh₄) (0.13 g, 0.10 mmol) in 1 mL of acetonitrile was added a solution of (Et₄N)(SPh) (0.096 g, 0.40 mmol) in 2 mL of acetonitrile to give a dark red-brown solution. Addition of 17 mL of THF

(30) Segal, B. M. Ph.D. Thesis, Harvard University, 2000.

Table 1. Crystallographic Data^a

param	4·MeCN	5	7	9	11·THF·2Et ₂ O
formula	C ₅₆ H ₁₀₂ ClFe ₄ NP ₃ S ₄	C ₆₀ H ₁₀₄ Fe ₄ P ₃ S ₅	C ₇₂ H ₁₁₄ Fe ₈ P ₄ S ₁₀ Si ₂	C ₅₄ H ₁₂₆ Fe ₈ P ₆ S ₈	C ₁₅₆ H ₂₉₂ Fe ₁₆ O ₃ P ₈ S ₁₆
cryst syst	orthorhombic	monoclinic	triclinic	triclinic	monoclinic
fw	1269.39	1302.04	1927.09	1664.65	3870.22
space group	<i>Pnma</i>	<i>P2₁/c</i>	<i>P1</i>	<i>P1</i>	<i>C2/c</i>
<i>a</i> , Å	19.982(2)	21.648(1)	11.2319(7)	19.982(2)	30.095(2)
<i>b</i> , Å	21.036(3)	15.6065(8)	13.600(8)	21.036(3)	20.362(2)
<i>c</i> , Å	15.508(4)	19.438(1)	15.382(9)	15.508(4)	34.992(3)
α, deg	90.	90.	82.051(1)	72.603(2)	90.
β, deg	90.	91.015(1)	80.924(1)	67.513(2)	111.092(1)
γ, deg	90.	90.	71.375(1)	80.848(3)	90.
<i>V</i> , Å ³	6473(2)	6566.1(6)	2189.2(2)	1936.6(4)	20006(2)
<i>Z</i>	4	4	1	1	4
ρ _{calc} , g cm ⁻³	1.303	1.317	1.462	1.427	1.285
2θ range, deg	3.34–55.9	3.22–45.0	2.70–56.6	3.30–45	2.48–45.0
GOF (<i>F</i> ²)	1.017	1.066	1.043	1.062	1.039
R1 ^{b,d} /R1 ^{c,d}	0.034/0.054	0.035/0.046	0.041/0.053	0.060/0.096	0.055/0.082
wR2 ^{b,e} /wR2 ^{c,e}	0.086/0.095	0.087/0.092	0.098/0.104	0.142/0.163	0.150/0.168

^a Obtained with graphite-monochromatized Mo Kα ($\lambda = 0.71071 \text{ \AA}$) radiation at 213 K. ^b Denotes value for the residual considering only the reflections with $I > 2\sigma(I)$. ^c Denotes value of the residual considering all the reflections. ^d $R1 = \sum(|F_o| - |F_c|)/\sum|F_o|$. ^e $wR2 = \{\sum[w(F_o^2 - F_c^2)^2]/\sum[w(F_o^2)^2]\}^{1/2}$; $w = 1/[\sigma^2(F_o^2) + (aP)^2 + bP]$, $P = [\max(F_o^2 \text{ or } 0) + 2(F_c^2)]/3$.

Chart 1. Designation of Clusters and Abbreviations

[Fe ₂ S ₄ (PR ₃) ₄] ¹⁺	1 (R = Pr'), 2 (R = Cy), 3 (R = Bu')
[Fe ₄ S ₄ (PCy ₃) ₃ Cl]	4
[Fe ₄ S ₄ (PCy ₃) ₃ (SPh)]	5
[Fe ₄ S ₄ (PPR ₃) ₃ (SSiPh ₃)]	6
[Fe ₈ S ₈ (PPR ₃) ₄ (SSiPh ₃) ₂]	7
[Fe ₄ S ₄ (PPR ₃) ₄]	8
[Fe ₈ S ₈ (PPR ₃) ₆]	9
[Fe ₁₀ S ₁₆ (PR ₃) ₈]	10 (R = Pr'), 11 (R = Cy), 12 (R = Bu')
[Fe ₄ S ₄ (SPh) ₄] ³⁻	13
[Fe ₄ S ₄ (S- <i>p</i> -tol) ₄] ³⁻	14
[Fe ₄ S ₄ (SPh) ₄] ⁴⁺	15

Abbreviations: Cy = cyclohexyl, S-*p*-tol = *p*-tolylthiolate(1-)

caused separation of the product as 0.064 g (75%) of fine black needles. The compound was identified by its ¹H NMR spectrum:^{2,31} δ 1.58 (*p*-H), 2.31 (*o*-H), 10.5 (*m*-H) (CD₃CN, anion).

(Et₄N)₃[Fe₄S₄(S-*p*-tol)₄]. The previous preparation was used but with 0.10 g (0.39 mmol) of (Et₄N)(S-*p*-tol). The product was obtained as 0.070 g (77%) of a black crystalline solid. The compound was identified by its ¹H NMR spectrum:³² δ 2.22 (*o*-H), 7.58 (*p*-CH₃), 10.4 (*m*-H) (CD₃CN, anion).

In the sections that follow, clusters are numerically designated as in Chart 1.

X-ray Structure Determinations. Diffraction data were acquired with a Siemens (Bruker) SMART CCD-based diffractometer; crystals were mounted on glass fibers and maintained under a stream of dinitrogen at 213 K. Cell parameters were retrieved using SMART software and refined using SAINT on all observed reflections. Data were collected using 0.3° intervals in θ and ω for 30 s/frame such that a hemisphere of data was collected. A total of 1271 frames were collected with a maximum resolution of 0.75 Å. The first 50 frames were recollected at the end of the data collection to monitor for decay; none was found. The highly redundant data sets were reduced using SAINT and corrected for Lorentz and polarization effects. Absorption corrections were applied using SADABS supplied by Bruker. Structures were solved by direct

methods using the program SHELXL-97. The positions of the metal atoms and their first coordination sphere were located from a direct-methods *E*-map; other non-hydrogen atoms were found in alternating difference Fourier syntheses and least-squares refinement cycles and, during the final cycles, were refined anisotropically. Hydrogen atoms were placed in calculated positions employing a riding model with thermal parameters 1.2 times of those of the bonded carbon atoms for all the methylene groups and 1.5 times for the methyl groups. Crystallographic data are collected in Table 1.³³

Black blocks of 4·MeCN were grown from acetonitrile/THF. The structure was solved in orthorhombic space group *Pnma* with *Z* = 4. The asymmetric unit contains half of cluster 4 and half acetonitrile molecule, which is disordered over two positions with equal occupancy. One of the cyclohexyl rings in a phosphine ligand is also disordered over two superimposed positions with approximately half-occupancy for each orientation. Black blocks of 5 were obtained from acetonitrile/THF; they occur in monoclinic space group *P2₁/c* with *Z* = 4. The asymmetric unit contains one molecule. Black needles of 7 were obtained from THF/ether vapor diffusion. The compound crystallizes in triclinic space group *P1* with *Z* = 1; the asymmetric unit contains half of the molecule. Black blocks of 9 were produced by layering a THF/PPR₃ solution of 8 with acetonitrile and maintaining the mixture at room temperature for 3 d. The cluster resides on an inversion center in triclinic space group *P1* with *Z* = 1; the asymmetric unit consists of half of the molecule. Black rhombic plates of 11·THF·2Et₂O were grown by THF/ether vapor diffusion. The compound occurs in monoclinic space group *C2/c* with *Z* = 4; the molecule resides on a 2-fold axis.

Other Physical Measurements. All measurements were performed under anaerobic conditions. Absorption spectra were recorded with a Varian Cary 50 Bio spectrophotometer. ¹H NMR spectra were recorded on a Bruker AM 400 or a Varian Mercury 300 spectrometers. Electrochemical measurements were made with a PAR model 263 potentiostat/galvanostat using a Pt working electrode, a 0.1 M (in dichloromethane)/0.2 M (in THF) (Bu₄N)⁺(PF₆)⁻ supporting electrolyte, and an SCE reference electrode. Mössbauer spectra were collected with a constant-acceleration spectrometer. Data were analyzed using WMOSS software (WEB Research Co., Edina, MN); isomer shifts are referenced to iron metal

(31) Reynolds, J. G.; Laskowski, E. J.; Holm, R. H. *J. Am. Chem. Soc.* **1978**, *100*, 5315–5322.

(32) Reynolds, J. G.; Coyle, C. L.; Holm, R. H. *J. Am. Chem. Soc.* **1980**, *102*, 4350–4355.

(33) See paragraph at the end of this article for Supporting Information available.

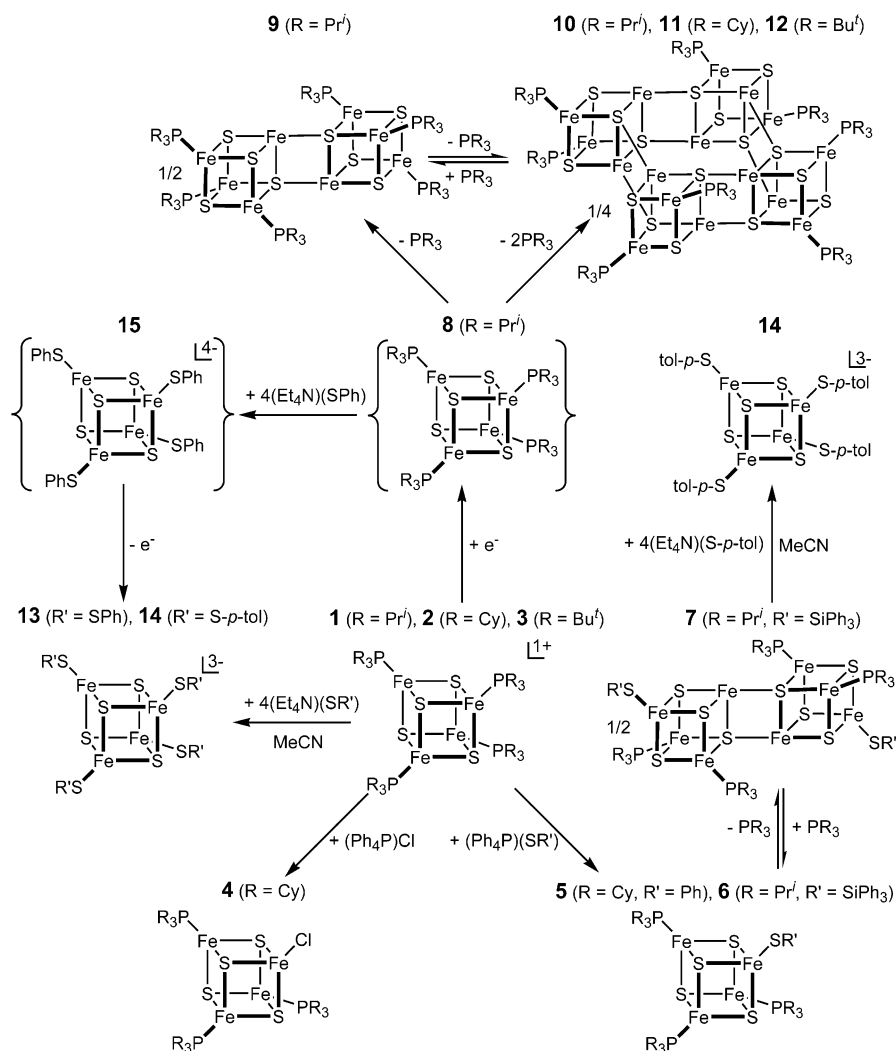


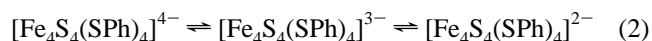
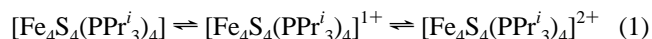
Figure 1. Summary of conversion reactions of iron–sulfur–phosphine clusters of nuclearities 4 (**1–6**, **8**, **13–15**), 8 (**7**, **9**), and 16 (**10–12**) arising from precursor single cubanes **1–3**. The species in parentheses have not been isolated; cluster **15** has not been definitely identified.

at room temperature. EPR spectra were recorded on a Bruker ESP 300-E spectrometer operating at X-band frequencies. Spectral simulations were performed with WIN-EPR SimFonia v. 1.25 software.

Results and Discussion

The principal results of this investigation are summarized by the reaction scheme in Figure 1. The scheme is entered via the clusters $[\text{Fe}_4\text{S}_4(\text{PR}_3)_4]^+$ (**1–3**), several of which have been reported earlier.⁹ It includes a variety of other single cubanes (**4–6**, **8**, **13–15**), dicubanes (**7**, **9**), and tetracubanes (**10–12**). Single cubanes **1–3** are prepared by the reaction of $[\text{Fe}_4\text{S}_4\text{Cl}_4]^{2-}$ with a tertiary phosphine having a cone angle of $\geq 160^\circ$.³⁴ The smaller cone angle of 130° for PET_3 leads to the formation of basket clusters.^{5,6} The limits of phosphine basicity and cone angle for exclusive formation of cubane-type clusters have not been ascertained. However, we have never encountered the basket structure with PPr_3 , whose cone angle of 160° is the smallest utilized in this and past work.^{9,26} Core reduction in the synthesis of **1–3** is effected by oxidation of phosphine, expressible by the formal half-reaction $\text{R}_3\text{P} + \text{S}^{2-} \rightleftharpoons \text{R}_3\text{PS} + 2\text{e}^-$.¹¹ The cluster $[\text{Fe}_4\text{S}_4(\text{PPr}_3)_4]^+$ is the most useful precursor cluster because of the

favorable solubility properties of neutral clusters derived from it. It supports the reversible three-member electron-transfer series (**1**) with $E_{1/2} = -0.99$ and 0.16 V in dichloromethane.⁹ When compared to the classical isoelectronic series (**2**) with $E_{1/2} = -1.72$ and -1.00 V in acetonitrile,³⁵ the stabilization amounts to 0.73 and 1.16 V, respectively. We consider next the various cluster transformations in Figure 1. A characteristic of most clusters shown is lability of the phosphine ligands, a property that can cause difficulty in achieving analytical purity in certain cases. Experimental procedures for clusters **1** and **9–12** represent substantial improvements over earlier methods⁹ and should be followed closely to obtain optimal yields and purity.



Monocubanes with the $[\text{Fe}_4\text{S}_4]^+$ Core. Cluster **1** is readily recognized by its ^1H NMR spectrum in Figure 2 with methine and methyl resonances at 5.05 and 2.29 ppm, respectively; this spectrum serves to differentiate it from other clusters

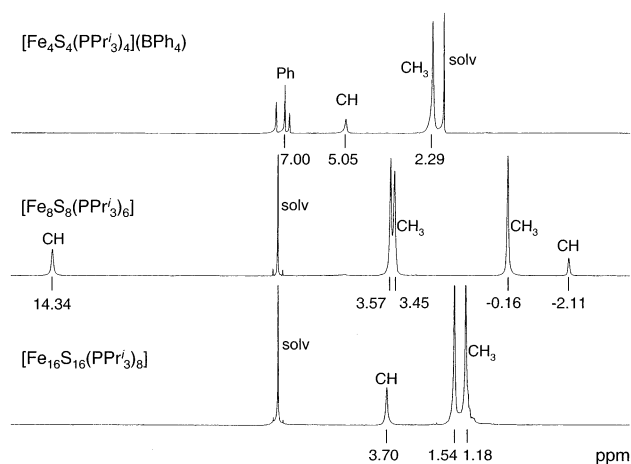
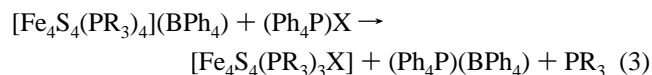


Figure 2. ^1H NMR spectra of $[\text{Fe}_4\text{S}_4(\text{PPR}'_3)_4](\text{BPh}_4)$ in CD_3CN (top) and $[\text{Fe}_8\text{S}_8(\text{PPR}'_3)_6]$ (middle) and $[\text{Fe}_{16}\text{S}_{16}(\text{PPR}'_3)_8]$ (bottom) in C_6D_6 . Signal assignments are indicated; solv = solvent.

with homoleptic PPR'_3 ligation (vide infra). Monosubstituted clusters **4**–**6** are obtainable in yields of 48%, 32%, and ~85% by reaction 3.



This reaction takes advantage of the insolubility of $(\text{Ph}_4\text{P})\text{X}$ in toluene, in which the neutral cluster products are freely soluble. Cluster **6** was identified by its ^1H NMR spectrum; it was not obtained in analytical purity but serves as a useful precursor of a dicubane (vide infra). Clusters **4** and **5** were obtained in pure form and were further identified by X-ray structure determinations. Structures are shown in Figure 3 together with Fe–Cl/SPh and mean Fe–S, Fe–Fe, and Fe–P bond distances. In chloride cluster **4**, Fe–S distances sort into sets of six short and six long. The independent short distances are Fe(1)–S(1) and Fe(2)–S(2,3) (2.261(1)–2.264(1) Å, mean 2.262(2) Å). The remaining distances are long (2.288(7)–2.332(1) Å, mean 2.30(2) Å)

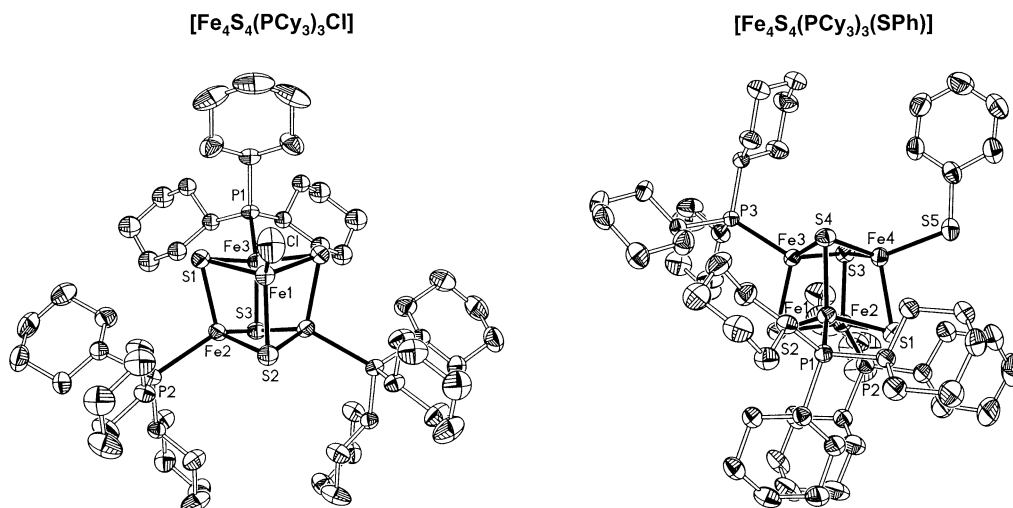


Figure 3. Structures of $[\text{Fe}_4\text{S}_4(\text{PCy}_3)_3\text{X}]$ showing 50% probability ellipsoids and partial atom labeling schemes. Selected bond lengths (Å) are summarized. X = Cl^- (left): Fe(3)–Cl 2.221(1), Fe–S 2.262(2) (mean of 3), 2.30(2) (mean of 4); Fe–Fe 2.69(1) (mean of 4); Fe–P, 2.38(1) (mean of 2). X = PhS^- (right): Fe(4)–S(5) 2.261(1); Fe–S 2.26(1) Å (mean of 8), 2.31(1) Å (mean of 4); Fe–Fe 2.68(1) (mean of 4); Fe–P 2.37(2) (mean of 3). The former structure has crystallographically imposed mirror symmetry.

Table 2. Zero-Field Mössbauer Parameters at 4.2 K

cluster	δ , mm/s	ΔE_Q , mm/s	% ^b
$[\text{Fe}_4\text{S}_4(\text{PCy}_3)_3\text{Cl}]^a$	0.49	1.16	75
	0.52	0.49	25
$[\text{Fe}_8\text{S}_8(\text{PPR}'_3)_4(\text{SSiPh}_3)_2]$	0.56	1.18	75
	0.40	0.45	25
$[\text{Fe}_8\text{S}_8(\text{PPR}'_3)_6]$	0.64	0.94	75
	0.53	2.49	25
$[\text{Fe}_{16}\text{S}_{16}(\text{PPR}'_3)_8]$	0.64	1.10	75
	0.55	2.63	25
$[\text{Fe}_{16}\text{S}_{16}(\text{PBu}'_3)_8]$	0.64	1.09	75
	0.58	2.68	25

^a 150 K. ^b Fits constrained with these percent absorptions.

and are placed to conform with the imposed mirror symmetry of the cluster. In benzenethiolate cluster **5**, Fe–S distances divide into sets of eight short (2.248(1)–2.276(1) Å, mean 2.26(1) Å) and four long (2.302(1)–2.333(1) Å, mean 2.312 Å). No symmetry is imposed on this cluster; the eight short distances occur in the Fe(3,4)S(3,4) and Fe(1,2)S(1,2) core faces. These clusters have $S = 1/2$ ground states, as indicated by the frozen-solution EPR spectrum of **4** ($g_{\perp} = 1.96$, $g_{\parallel} = 2.13$; not shown), and one reversible redox step in dichloromethane at $E_{1/2} = -1.07$ V (**4**) and -1.06 V (**5**) corresponding to the $[\text{Fe}_4\text{S}_4(\text{PCy}_3)_3\text{X}]^{0/-}$ couple. Mössbauer spectral parameters for **4** and other phosphine-ligated clusters are listed in Table 2. At 150 K the spectrum of **4** consists of two overlapping quadrupole doublets which were fitted in a 3:1 intensity ratio. The more intense doublet has $\delta = 0.49$ mm/s and $\Delta E_Q = 1.16$ mm/s, and the less intense doublet, $\delta = 0.52$ mm/s and $\Delta E_Q = 0.49$ mm/s. The mean isomer shift (0.50 mm/s, 150 K) is closely comparable to that of isoelectronic $[\text{Fe}_4\text{S}_4(\text{PCy}_4)_4]^+$ (0.48 mm/s, 77 K).⁹ The unique site is associated with chloride and might be expected to have more Fe^{III} character and a lower isomer shift. However, the intrinsic chemical shift order $\text{X} = \text{Cl}^- > \text{RS}^- > \text{PR}_3$ for tetrahedral $\text{Fe}_4\text{S}_4\text{X}$ sites^{11,12} may obscure this effect.

Clusters **4**–**6** are 3:1 site-differentiated single cubanes prepared without recourse to a site-differentiating ligand. Their formation and resistance to disproportionation arises

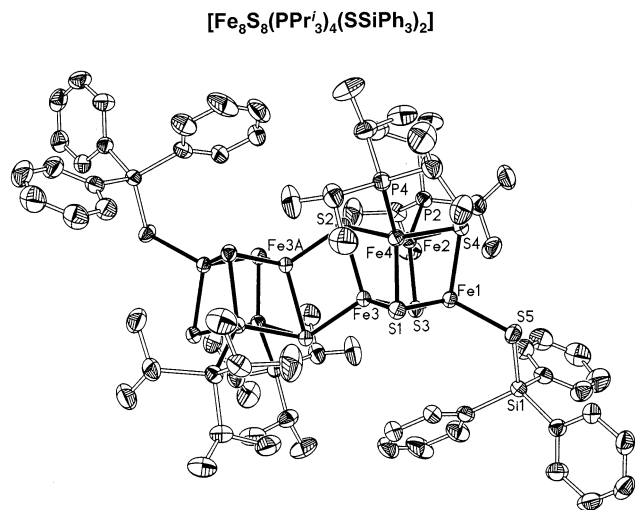


Figure 4. Structure of $[\text{Fe}_8\text{S}_8(\text{PPr}^i_3)_4(\text{SSiPh}_3)_2]$ showing 50% probability ellipsoids and a partial atom labeling scheme. The structure has a crystallographically imposed inversion center. Selected bond lengths (Å) and angles (deg) are summarized. Cube: Fe(1)–S(5) 2.248(1), Fe–S 2.28(1) (mean of 9, excluding Fe(2–4)–S(2)), Fe(2–4)–S(2) 2.38(3) (mean of 3), Fe(1)–Fe(2–4) 2.75(2) (mean of 3); Fe(2)–Fe(3,4), Fe(3)–Fe(4), 2.60(1) (mean of 3). Bridge rhomb: Fe(3)–S(2) 2.417(8), Fe(3)–S(2A) 2.269(1), Fe(3)–Fe(3A) 2.788(1), Fe(3)–S(2)–Fe(3A) 74.92(4), S(2)–Fe(3)–S(2A) 107.06(2).

from the use of near-stoichiometric reactants in reaction 3 and low-polarity media as reaction and purification solvents for the uncharged clusters. The related $S = 1/2$ clusters $[\text{Fe}_4\text{S}_4(\text{PBU}^i_3)_3\text{X}]$ ($\text{X} = \text{halide}$) were prepared first by the reaction of $[\text{Fe}_4\text{S}_4\text{X}_4]^{2-}$ in acetonitrile with PBU^i_3 in THF followed by addition of NaBPh_4 .¹⁰ The authenticity of these clusters is not in question; indeed, the structure of **4** compared closely with $[\text{Fe}_4\text{S}_4(\text{PBU}^i_3)_3\text{Cl}]$. However, in our hands this procedure, with bulky phosphines, affords **1–3** rather than monosubstituted clusters. The scope of reaction 3 should be extendable to other $[\text{Fe}_4\text{S}_4(\text{PR}^i_3)_3\text{X}]$ clusters. Last, during exploration of synthetic methods for single cubanes, we found that $[\text{Fe}_4\text{S}_4(\text{PPr}^i_3)_3(\text{SPh})]$ (38%) could be prepared in the complicated assembly system $[\text{FeCl}_2(\text{PET}_3)_2]/\text{NaSPh}/(\text{PhCH}_2\text{S})_2\text{S}/\text{PPr}^i_3$ in toluene.³⁰ The scope of this procedure was not investigated.

Dicubane with the $[\text{Fe}_8\text{S}_8]^{2+}$ ($2[\text{Fe}_4\text{S}_4]^+$) Core. Under anaerobic conditions in a low-polarity solvent like THF or toluene, monocubanes **4** and **5** are stable. However, when ether is added by diffusion to a solution of silanethiolate cluster **6** in THF, reaction 4 occurs with the separation of the less soluble cluster **7** (73%), whose structure is shown in Figure 4. Because the structure is very similar to that of $[\text{Fe}_8\text{S}_8(\text{PPr}^i_3)_6]$, described in detail below, a limited set of metric parameters is included in the figure legend. The centrosymmetric edge-bridged dicubane arrangement with a 2:4:2 population of iron sites in the $[\text{Fe}_8\text{S}_8]^{2+}$ core is immediately evident. Formation of bridge rhomb Fe(3,3A)–S(2,2A) elongates the Fe(2–4)–S(2) bonds (mean 2.38(3) Å) relative to nine other Fe–S bonds in the cubane unit (mean

(34) Woska, D.; Prock, A.; Giering, W. P. *Organometallics* **2000**, *19*, 4629–4638.

(35) Cambray, J.; Lane, R. W.; Wedd, A. G.; Johnson, R. W.; Holm, R. H. *Inorg. Chem.* **1977**, *16*, 2565–2571.

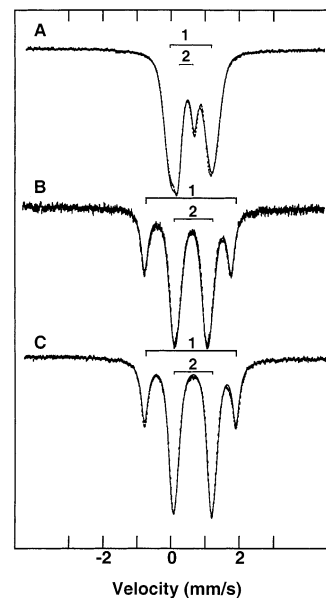
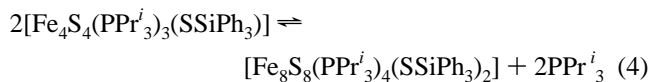


Figure 5. Zero-field Mössbauer spectra at 4.2 K of polycrystalline $[\text{Fe}_8\text{S}_8(\text{PPr}^i_3)_4(\text{SSiPh}_3)_2]$ (A), $[\text{Fe}_8\text{S}_8(\text{PPr}^i_3)_6]$ (B), and $[\text{Fe}_{16}\text{S}_{16}(\text{PPr}^i_3)_8]$ (C). Solid lines are fits to the data using the parameters of Table 2.

2.28(1) Å). In the plane Fe(2,3,4) the three Fe–Fe distances are much shorter (mean 2.60(1) Å) than the remaining three such distances (2.75(2) Å). The bridge rhomb is characterized by edges of 2.417(1) (Fe(3)–S(2)) and 2.269(1) Å (Fe(3)–S(2A)), a diagonal distance of 2.788(1) Å (Fe(3)–Fe(3A)), and angles of 107.06(2)° (S(2)–Fe(3)–S(2A)) and 72.94° (Fe(3)–S(2)–Fe(3A)). As is the case with double cubanes having Fe_8S_8 ,⁹ $\text{V}_2\text{Fe}_6\text{S}_8$,¹² and $\text{Mo}_2\text{Fe}_6\text{S}_8$ ^{11,13,14,19} cores, the Fe–S intercubane bond is significantly shorter than the Fe–S intracubane bond within the rhomb, here by 0.15 Å. The reason for this behavior is unclear. The edge-bridged double cubane motif, while still uncommon, is found in a six-coordinate Fe_8S_8 cluster³⁶ and in $\text{Mo}_6\text{Cu}_2\text{S}_8$,³⁷ $\text{Mo}_6\text{Pd}_2\text{S}_8$,³⁸ $\text{Mo}_2\text{W}_4\text{Ni}_2\text{S}_8$,³⁹ and $\text{W}_6\text{Ni}_2\text{S}_8$ ^{39,40} clusters. In the heterometal species enumerated here, the last-named metal is involved in the rhomb bridge.



The Mössbauer spectrum of dicubane **7**, set out in Figure 5A, consists of two overlapping quadrupole doublets; parameters are given in Table 2. The three types of iron atoms are not resolved. The more intense doublet with $\delta = 0.56$ mm/s is more “ferrous-like” and contains the four FeS_3P sites and the two bridging iron atoms. The less intense doublet with $\delta = 0.40$ mm/s indicates more ferric character and is ascribed to the iron thiolate site. The average isomer

(36) Harmjan, M.; Saak, W.; Pohl, S. *J. Chem. Soc., Chem. Commun.* **1997**, 951–952.

(37) Shibahara, T.; Akashi, H.; Kuroya, H. *J. Am. Chem. Soc.* **1988**, *110*, 3313–3314.

(38) Murata, T.; Gao, H.; Mizobe, Y.; Nakano, F.; Motomura, S.; Tanase, T.; Yano, S.; Hidai, M. *J. Am. Chem. Soc.* **1992**, *114*, 8287–8288.

(39) Shibahara, T.; Sakane, G.; Maeyama, M.; Kobashi, H.; Yamamoto, T.; Watase, T. *Inorg. Chim. Acta* **1996**, *251*, 207–225.

(40) Shibahara, T.; Yamamoto, T.; Sakane, G. *Chem. Lett.* **1994**, 1231–1234.

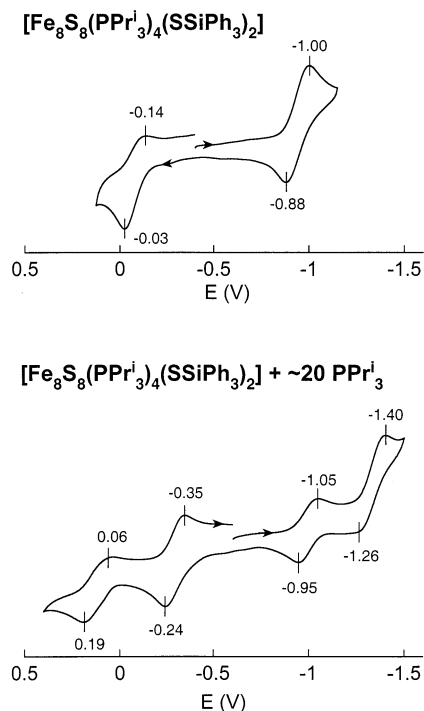
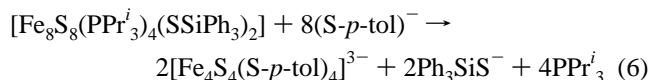
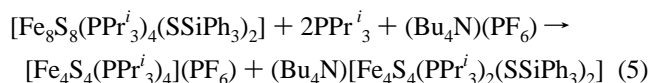


Figure 6. Cyclic voltammograms (100 mV/s) of 1.9 mM $[\text{Fe}_8\text{S}_8(\text{PPri}_3)_4(\text{SSiPh}_3)_2]$ (top) and in the presence of ~ 20 equiv of PPr_3 (bottom). Peak potentials are indicated.

shift of 0.52 mm/s is compatible with $\delta = 0.59$ mm/s for $[\text{Fe}_4\text{S}_4(\text{SEt})_4]^{3-41}$ when the ligand chemical shift effect (noted above) is taken into account.

A series of reactions were performed to assess the stability of the double cubane structure to attack by nucleophiles. It was first found that reaction 4 is readily reversible. When monitored by ^1H NMR, addition of excess phosphine to a 1.0 mM solution of dicubane **7** (δ 3.21 (br, Me)) in dichloromethane results in formation of monocubane **6** (δ 2.14 (Me), 3.56 (CH)). With 8 equiv of phosphine, complete conversion to **6** occurs in 16 h. When monitored by cyclic voltammetry in dichloromethane in the presence of ~ 20 equiv of phosphine and 0.1 M supporting electrolyte, reaction 5 occurs. As seen in Figure 6, dicubane **7** exhibits one reduction and one oxidation step at $E_{1/2} = -0.94$ and -0.09 V, respectively, in the three-member series $[\text{Fe}_8\text{S}_8(\text{PPri}_3)_4(\text{SSiPh}_3)_2]^{+/0/-}$. In the presence of ~ 20 equiv of phosphine, four new redox steps develop. Those at +0.13 and -1.00 V are due to $[\text{Fe}_4\text{S}_4(\text{PPr}_3)_4]^+$. The remaining features do not arise from **6** or **7**. They are assigned to the indicated monoanion which forms the three-member series $[\text{Fe}_4\text{S}_4(\text{PPr}_3)_2(\text{SSiPh}_3)_2]^{0/-/2-}$ with $E_{1/2} = -0.30$ and -1.33 V. While it could be fortuitous, we note the 1.03 V separation of potentials is similar to that (1.13 V) for isoelectronic redox series 1. Potentials are more negative owing to the larger negative charge on the clusters. Reaction 5 is written so as to indicate the stabilization of charged reaction products in a low dielectric medium by a high concentration of counterions; it does not imply complete ion pairing. Last, treatment of **7** with 8 equiv of $(\text{Et}_4\text{N})(\text{S}-p\text{-tol})$ in acetonitrile

causes complete conversion to $[\text{Fe}_4\text{S}_4(\text{S}-p\text{-tol})_4]^{3-}$ in reaction 6; the product cluster is unambiguously identified by its contact-shifted ^1H NMR spectrum.⁵¹



The preceding observations demonstrate that the edge-bridged dicubane structure of **7** is cleaved under mild conditions. Further, cleavage produces monocubane products, not other fragments of the parent cluster within our limits of detection by NMR and voltammetry. The source of the facile cleavage is not weak $\text{Fe}-(\mu_4\text{-S})$ bridge bonds (on the basis of their lengths) but, it is proposed, strain primarily located at the bridge atoms. The six angles $\text{S}-\text{Fe}(3)-\text{S}$ range from 102.9 to 115.7° , with four at or below 108.4° . While somewhat removed from the ideal tetrahedral angle, these angles are not the primary locus of strain. Bond angles at the $\mu_4\text{-S}(2)$ atom are far more contorted. Four $\text{Fe}-\text{S}(2)-\text{Fe}$ angles are in the narrow interval $65.5-72.9^\circ$; the two others are $\text{Fe}(3\text{A})-\text{S}(2)-\text{Fe}(2,4) = 124.96(3)$ and $125.72(3)^\circ$. Disruption of the bridge rhomb allows adoption of normal $\text{Fe}-(\mu_3\text{-S})-\text{Fe}$ angles. In cluster **5**, for example, the 12 such angles define the narrow range $71.13(3)-73.02(3)^\circ$. These angles are themselves strained from limiting $\text{S } sp^3$ (109.5°) or p^3 (90°) reference configurations, but the existence of several hundred synthetic $[\text{Fe}_4\text{S}_4]^{2+,+}$ monocubanes is ample testimony to the viability of a set of ostensibly strained angles in a stable structure. In the present context, the apparent tradeoff is six strained bond angles for four in two stable structures.

Monocubanes with the $[\text{Fe}_4\text{S}_4]^0$ Core. Previously, we had shown that reduction of clusters **1-3** with sodium acenaphthylenide in THF generates the neutral clusters $[\text{Fe}_4\text{S}_4(\text{PR}_3)_4]$ with an all-ferrous core.⁹ Attempts to isolate these clusters in substance failed. Here we have concentrated on the triisopropylphosphine cluster **8** and its more soluble oligomers in a broader range of experiments. Reaction 7 with cluster **1** and the strong reductant potassium benzophenone ketyl (ca. -1.8 V vs SCE in THF⁴²) was extensively investigated under a variety of conditions with variable excess amounts of PPr_3 . When reaction 7 was carried out in THF in the presence of 23 equiv of phosphine, the formation of **8** was consistent with the results of FAB mass spectrometry, which detected the parent ion and fragments resulting from the stepwise loss of one to four phosphine ligands. Volume reduction in vacuo of a reaction solution results mainly in the loss of THF (bp 66°C) and formation of an oily residue. Continuation of the procedure removes PPr_3 (bp 176°C) and affords a black solid whose composition appears to depend on the amount of phosphine added. With ≥ 18 equiv, the main product is the dicubane **9**. With 3–18 equiv, a mixture of **9** and tetracubane **10** is obtained.

(41) Zhou, H.-C.; Su, W.; Achim, C.; Rao, P. V.; Holm, R. H. *Inorg. Chem.* **2002**, *41*, 3191–3201.

(42) Connelly, N. G.; Geiger, W. E. *Chem. Rev.* **1996**, *96*, 877–910.

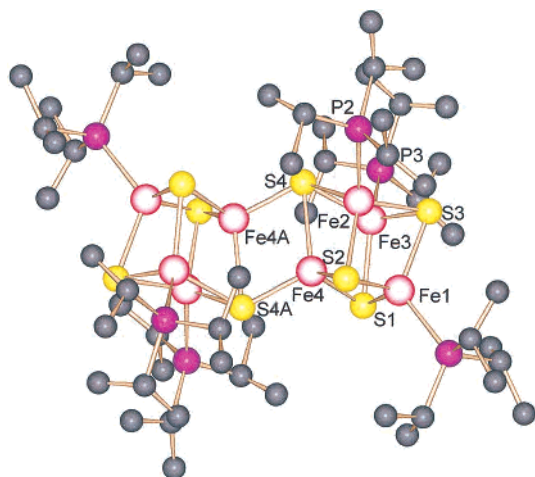
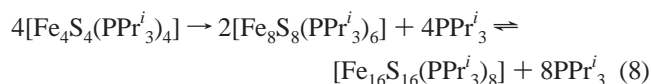
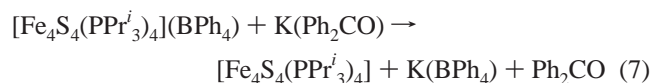


Figure 7. Structure of $[\text{Fe}_8\text{S}_8(\text{PPr}_3)_6]$ showing a partial atom labeling scheme and presented in a ball-and-stick motif for clarity. Atoms are represented by spheres of arbitrary radius. The structure has a crystallographically imposed inversion center.

In the presence of 2.7 equiv, **10** is isolated as the sole product. When monocubane **1** was reduced in the absence of phosphine, an uncharacterized black product was obtained. These observations are summarized by the reaction scheme in eq 8.



Clusters **9** and **10** were identified by the ^1H NMR spectra shown in Figure 2. In this work as well, we have been unable to devise conditions leading to the isolation of an all-ferrous monocubane. Conversion to **9** and **10** is assisted by removal of phosphine and the much lower solubilities of these clusters in THF, benzene, and toluene. We conclude that monocubane **8** is stable only in solution.

Dicubane with the $[\text{Fe}_8\text{S}_8]^0$ ($2[\text{Fe}_4\text{S}_4]^0$) Core. The all-ferrous dicubane $[\text{Fe}_8\text{S}_8(\text{PCy}_3)_6]$ has been previously reported.^{9,26} However, the utility of this compound is diminished by its virtual insolubility in common organic solvents.⁴³ The more soluble cluster **9** is readily prepared by layering a solution of **8** and 27 equiv of triisopropylphosphine in THF with 18 equiv of phosphine in a larger volume of acetonitrile. Under these conditions, dicubane **9** has been reproducibly isolated in 60% yield. Its structure, presented in Figure 7, has imposed centrosymmetry and idealized C_{2h} symmetry and is more accurate than that of $[\text{Fe}_8\text{S}_8(\text{PCy}_3)_6]$, which was not reported in detail.²⁶ Consequently, Table 3, containing selected distances and angles, is included. Because the core structure is highly similar to that of **7**, no detailed discussion is required. Patterns of bond distances and angles are retained with small changes in dimensions. For example, in the bridge

Table 3. Selected Interatomic Distances (Å) and Angles (deg) for $[\text{Fe}_8\text{S}_8(\text{PPr}_3)_6]$

Fe(4)–S(4)	2.401(2)	S(4)–Fe(4)–S(4A)	108.33(7)
Fe(4)–S(4A)	2.320(2)	Fe(4)–S(4)–Fe(4A)	71.67(7)
Fe(4)–Fe(4A)	2.765(2)		
Fe(2)–S(4)	2.386(2)	Fe(2)–S(4)–Fe(3)	64.57(6)
Fe(3)–S(4)	2.373(2)	Fe(4)–S(4)–Fe(2)	66.14(7)
Fe(4)–S(1)	2.319(2)	Fe(4)–S(4)–Fe(3)	66.67(6)
Fe(4)–S(2)	2.321(3)		
		S(1)–Fe(4)–S(2)	104.58(8)
Fe(2)–S(2)	2.291(2)	S(1)–Fe(4)–S(4)	107.50(9)
Fe(2)–S(3)	2.309(2)	S(2)–Fe(4)–S(4)	108.00(9)
Fe(3)–S(1)	2.296(3)	S(1)–Fe(1)–S(3)	104.35(9)
Fe(3)–S(3)	2.321(3)	S(1)–Fe(1)–S(2)	107.40(9)
		S(2)–Fe(1)–S(3)	104.23(9)
Fe(4)–Fe(1)	2.699(2)	S(2)–Fe(2)–S(3)	103.86(8)
Fe(4)–Fe(2)	2.612(2)	S(2)–Fe(2)–S(4)	109.55(9)
Fe(4)–Fe(3)	2.624(2)	S(3)–Fe(2)–S(4)	111.43(9)
Fe(1)–Fe(2)	2.705(2)	S(1)–Fe(3)–S(3)	103.20(9)
Fe(1)–Fe(3)	2.720(2)	S(1)–Fe(3)–S(4)	109.24(8)
Fe(2)–Fe(3)	2.542(2)	S(3)–Fe(3)–S(4)	111.47(9)
Fe(1)–P(1)	2.335(2)	P–Fe–S	100.1(1)–118.6(1)
Fe(2)–P(2)	2.455(3)		
Fe(3)–P(3)	2.465(3)		

rhomb Fe(4,4A)S(4,4A) the intercubane Fe–S distance (2.320(2) Å) is shorter than the intracubane distance (2.401(2) Å), and the angles at μ_4 -S(4) divide into two large (125.3(1), 125.8(3)°) and four small (66.1–71.7°).

The isotropically shifted ^1H NMR spectrum of **9** (Figure 2) is consistent with a 2:1 population of phosphine-bound iron sites. The features at δ –0.16 and –2.11 are ascribed to sites on a idealized mirror plane containing the bridge rhomb; the remaining resonances arise from the four equivalent sites off the plane. Two methyl signals (δ 3.45, 3.57) derive from the diastereotopic nature of the methyl groups at these sites.

Tetracubane with the $[\text{Fe}_{16}\text{S}_{16}]^0$ ($4[\text{Fe}_4\text{S}_4]^0$) Core. Clusters **10–12** were prepared by the reduction of **1**(BPh₄) in THF in the presence of excess phosphine followed by layering the reaction mixture with acetonitrile and allowing the mixture to stand for varying periods. Yields of 55% (**10**), 45% (**11**), and 62% (**12**) were obtained. Cluster **11** is very slightly soluble, and clusters **10** and **12** are appreciably soluble in benzene, toluene, and THF.⁴³ The structure of **11** in a solvate crystal is presented in Figure 8. It consists of four cubane units, each bridged by two rhombs to form a cyclic structure which is chiral with a highest idealized symmetry of D_4 . Because of a crystallographic 2-fold axis, the actual symmetry is only C_2 . Owing to the large number of parameters, the variability of those of the same distance and angle type, and the similarity to dicubane **9**, metric data are not tabulated.³³ The pattern of distances and angles in the bridge rhomb and in the individual cubanes resembles **9**. The central part of the structure consists of four fused Fe_2S_2 rhombs in which the Fe–Fe separations alternate long and short. Proceeding from Fe(3A) clockwise, the distances are 2.736(2), 2.522(1), 2.728(1), and 2.526(1) Å with the longer distances in the bridge rhombs. The structure of $[\text{Fe}_{16}\text{S}_{16}(\text{PBu}^t_3)_8]$ has also been described in a solvate crystal with imposed C_4 symmetry; an extensive tabulation of dimensions, which are very similar to those of **11**, is available.⁹ The tetracubanes **10–12** and the two isomers of

(43) The solubilities of clusters **9**, **10**, and **12** in solvents such as THF, benzene, and toluene are much larger than originally reported.⁹ The slight or nil solubility of $[\text{Fe}_8\text{S}_8(\text{PCy}_3)_6]$ in these solvents was properly described. All of these clusters are essentially insoluble in acetonitrile.

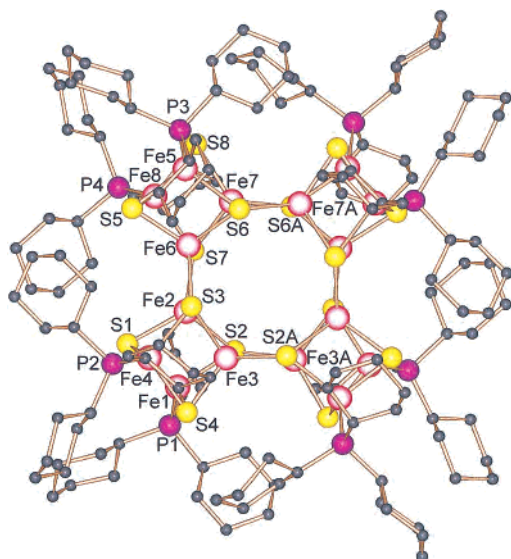


Figure 8. Structure of one enantiomer of $[\text{Fe}_{16}\text{S}_{16}(\text{PCy}_3)_8]$ showing a partial atom labeling scheme and presented in a ball-and-stick motif for clarity. Atoms are represented by spheres of arbitrary radius. The structure has a crystallographically imposed C_2 axis which passes through the center of rhombs $\text{Fe}(3,3\text{A})\text{S}(2,2\text{A})$ and $\text{Fe}(7,7\text{A})\text{S}(6,6\text{A})$.

$[\text{Na}_2\text{Fe}_{18}\text{S}_{30}]^{8-}$ ^{44,45} are the only known cyclic iron–sulfur clusters but differ in that cubane units and terminal ligands are absent in the latter.

Retention of the cyclic structure in benzene solution is demonstrated by the ^1H NMR spectrum of **10** (Figure 2). The spectrum, consisting of a single methine and two diastereotopic methyl signals, is indicative of the removal of crystalline constraints and the adoption of molecular D_4 symmetry with eight equivalent FeS_3P sites. As shown in Figure 9, **12** in THF exhibits three oxidation steps at $E_{1/2} = -0.57, -0.09,$ and $+0.22$ V, defining the four-member electron-transfer series $[\text{Fe}_{16}\text{S}_{16}(\text{PBu}'_3)_8]^{0/+2+/3+}$. In contrast, single cubane **3**, with the same terminal ligands, in the same solvent shows only a single step, a reduction at -0.75 V.

The Mössbauer spectra of clusters of dicubane **9** and tetracubanes **10** and **12** at 4.2 K consist of two resolved quadrupole doublets (Figure 5). Spectra were fitted to two doublets with the parameters in Table 2. While for **9**, with three different iron sites, assignment of the minority doublet to the bridging site ($\text{Fe}(4)$) might seem obvious, this assignment is questionable because the isomer shift of 0.53 mm/s is considerably below the usual 0.60–0.70 mm/s for tetrahedral $\text{Fe}^{\text{II}}\text{S}_4$.⁴⁶ For example, the isomer shift of the all-ferrous cluster $\text{Fe}_4\text{S}_4(\text{S}\cdot\text{Cys})_4$ of the iron protein of nitrogenase is 0.68 mm/s at 4.2 K.^{23,24} Further, this shift is smaller than for the FeS_3P sites, in disagreement with the chemical shift effect of anionic sulfur and phosphine ligands noted earlier. Clusters **10** and **12** contain two types of sites, 8 bridging FeS_4 and 8 FeS_3P . While those of the same type

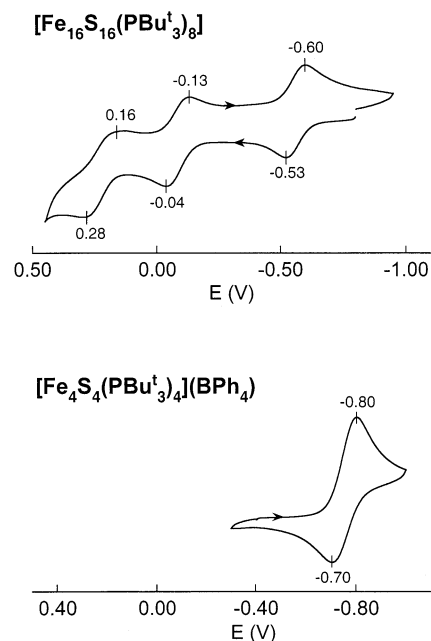


Figure 9. Cyclic voltammograms (100 mV/s) of $[\text{Fe}_{16}\text{S}_{16}(\text{PBu}'_3)_8]$ (top) and $[\text{Fe}_4\text{S}_4(\text{PBu}'_3)_4]^+$ (bottom) in THF. Peak potentials are indicated.

are not necessarily symmetry-equivalent in a crystal, the reasonable expectation of two doublets of equal intensity is not met. We note that the Mössbauer spectra were determined at 4.2 K and the crystal structures at 213 K. Spectra at higher temperatures became less resolved and were not useful in making assignments. Although definite assignment of the spectra is lacking, the average isomer shifts of 0.61–0.63 mm/s are fully consistent with the all-ferrous oxidation level.

Substitution Reactions of Monocubanes. Clusters **1–3** are viable starting materials for the preparation of other $[\text{Fe}_4\text{S}_4]^+$ monocubanes. As one example, reaction 9 proceeds readily in acetonitrile to afford the reduced clusters with $\text{R} = \text{Ph}$ (75%) and *p*-tol (77%) as pure Et_4N^+ salts after addition of THF. This reaction is similar to double cubane cleavage reaction 6; initial clusters have the same oxidation state. Reduced clusters are otherwise prepared by chemical reduction of $[\text{Fe}_4\text{S}_4(\text{SR})_4]^{2-}$,^{35,47} or by self-assembly.⁴⁸ Reaction 9 suggests the related process (10) in which a neutral phosphine cluster such as **8** is converted to a biologically relevant all-ferrous thiolate cluster $[\text{Fe}_4\text{S}_4(\text{SR})_4]^{4-}$. In a typical experiment, a freshly prepared solution of **8** and 2.2 equiv of PPr'_3 in THF was treated with 4.0 equiv of $(\text{Et}_4\text{N})(\text{SPh})$ in acetonitrile under rigorously anaerobic conditions. Addition of THF gave a black microcrystalline solid, which was isolated, washed, and dried. Its zero-field Mössbauer spectrum at 4.2 K (not shown) consists of two resolved quadrupole doublets in a 3:1 intensity ratio. The majority/minority doublets have $\delta = 0.67/0.68$ mm/s and $\Delta E_Q = 1.06/2.96$. The fully reduced cluster of the nitrogenase iron protein from *Azotobacter vinelandii* affords a closely related 3:1 doublet spectrum which was analyzed as four quadrupole

(44) You, J.-F.; Snyder, B. S.; Papaefthymiou, G. C.; Holm, R. H. *J. Am. Chem. Soc.* **1990**, *112*, 1067–1076.

(45) You, J.-F.; Papaefthymiou, G. C.; Holm, R. H. *J. Am. Chem. Soc.* **1992**, *114*, 2697–2710.

(46) Münck, E. In *Physical Methods in Inorganic and Bioinorganic Chemistry*; Que, L., Jr., Ed.; University Science Books: Sausalito, CA, 2000.

(47) Laskowski, E. J.; Frankel, R. B.; Gillum, W. O.; Papaefthymiou, G. C.; Renaud, J.; Ibers, J. A.; Holm, R. H. *J. Am. Chem. Soc.* **1978**, *100*, 5322–5337.

(48) Hagen, K. S.; Watson, A. D.; Holm, R. H. *Inorg. Chem.* **1984**, *23*, 2984–2990.

doublets with $\delta = 0.68$ mm/s and $\Delta E_Q = 3.08$ and 1.25–1.75 mm/s.^{23,24} When the solid was dissolved in CD₃CN, its ¹H NMR spectrum contains three signals at δ 4.64, 5.28 (br), and 9.43, which appear to be the contact-shifted *p*-H, *o*-H, and *m*-H resonances of a benzenethiolate cluster, and the *m*-H signal of [Fe₄S₄(SPh)₄]³⁻ (δ 10.5) in ca. 1.9:1 intensity ratio. The set of three is not due to the more oxidized members of series (2). In acetonitrile solution, the absorption spectrum of the solid affords a clear shoulder at ca. 560 nm, which may be the counterpart of the unusual 520 nm feature of the fully reduced protein. The collective results suggest that the isolated solid is the Et₄N⁺ salt of all-ferrous cluster **15** (Figure 1) or possibly of the edge-bridged double cubane [Fe₈S₈(SPh)₆]⁶⁻, which is expected to have a similar Mössbauer spectrum (cf. Figure 5B). The viability of this route to all-ferrous thiolate clusters is under further investigation. Definitive proof requires an X-ray structure determination.



Summary. The following are the principal results and conclusions of this investigation.

(1) A family of reduced iron–sulfur clusters with tertiary phosphine terminal ligands (cone angles $\geq 160^\circ$) and based on the cubane structural motif with nuclearities 4, 8, and 16 has been synthesized. The ultimate starting point is [Fe₄S₄Cl₄]²⁻, which is reductively substituted with phosphine to [Fe₄S₄(PR₃)₄]⁺ (R = Pr^{*i*}, Cy, Bu^{*t*}) from which other clusters are prepared. Improved preparations are given for certain clusters previously reported,^{9,25} and ⁵⁷Fe isomer shifts and X-ray structures have been determined for monosubstituted cubanes, dicubanes, and tetracubanes.

(2) Monocubane [Fe₄S₄(PR₃)₄]⁺ can be partially substituted to give neutral site-differentiated [Fe₄S₄(PR₃)₃X] (R = Cy, X = Cl⁻, RS⁻), fully substituted to form [Fe₄S₄(SR)₄]³⁻ (R = Ph, *p*-tol), and reduced to all-ferrous [Fe₄S₄(PR₃)₄], which could not be isolated in substance. The monosubstituted clusters show different distortions of the [Fe₄S₄]⁺ cores

from idealized cubic symmetry, a common feature of the clusters in this oxidation state.

(3) Dicubanes [Fe₈S₈(PPr^{*i*}₃)₄(SSiPh₃)₂] and [Fe₈S₈(PPr^{*i*}₃)₆] were prepared from [Fe₄S₄(PPr^{*i*}₃)₃(SSiPh₃)] and [Fe₄S₄(PPr^{*i*}₃)₄], respectively, and were shown to possess edge-bridged double cubane structures with an Fe₂(μ₄-S)₂ bridge rhomb in which the intercubane (bridging) Fe–S distance is shorter (0.15, 0.08 Å) than the intracubane Fe–S distance.

(4) Dicubane [Fe₈S₈(PPr^{*i*}₃)₄(SSiPh₃)₂] is readily cleaved with thiolate or PPr^{*i*}₃ to single cubanes in reactions that may be assisted by bond angle strain at the μ₄-S atoms.

(5) Tetracubanes [Fe₁₆S₁₆(PR₃)₈] are obtained from [Fe₄S₄(PR₃)₄]. The isolation of dicubanes and tetracubanes is assisted by their relatively low solubilities compared to [Fe₄S₄(PR₃)₄] in the presence of excess phosphine. Their cyclic structures are built of four cubane clusters, each of which forms two bridge rhombs with adjacent clusters. This structure is, thus far, unique among metal–sulfur clusters.

(6) Tertiary phosphines as ligands are devices that stabilize low oxidation states of iron–sulfur clusters, which in turn manifest dicubane and tetracubane structures not found with more oxidized clusters, and electron-transfer series of up to four members.

The species [Fe₄S₄(PR₃)₄] (solution), [Fe₈S₈(PR₃)₆], and [Fe₁₆S₁₆(PR₃)₈] are the only synthetic all-ferrous iron–sulfur clusters with tetrahedral metal sites that have been generated in solution or isolated in substance. These properties, together with favorable solubility and facile phosphine substitution, render them potentially attractive starting compounds for the generation of reduced clusters of nuclearity four and higher. This matter is currently under investigation.

Acknowledgment. This research was supported by NIH Grant 28856. We thank Drs. B. M. Segal, C. Achim, and P. Venkateswara Rao for experimental assistance and useful discussions.

Supporting Information Available: Tables of positional and thermal parameters and bond lengths and angles for the five compounds in Table 1 in CIF format. This material is available free of charge via the Internet at <http://pubs.acs.org>.

IC020464T